



Electrochemical and microbial community responses of electrochemically active biofilms to copper ions in bioelectrochemical systems



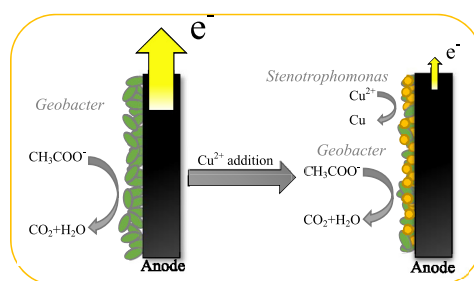
Yaping Zhang, Guanqun Li, Jing Wen, Yangao Xu, Jian Sun, Xun-an Ning, Xingwen Lu, Yujie Wang, Zuoyi Yang, Yong Yuan*

School of Environmental Science and Engineering, Institute of Environmental Health and Pollution Control, Guangdong University of Technology, Guangzhou 510006, PR China

HIGHLIGHTS

- Cu^{2+} caused EABs damage and decreased secretion of outer membrane cytochromes.
- The flow of electrons could improve the reduction of copper.
- The recovery capability of EABs was higher compared to nonelectroactive bacteria.
- A decrease in *Geobacter* accompanied by an increase in *Stenotrophomonas* was observed.

GRAPHICAL ABSTRACT



ARTICLE INFO

Article history:

Received 27 October 2017

Received in revised form

23 December 2017

Accepted 4 January 2018

Available online 5 January 2018

Handling Editor: E. Brillas

Keywords:

Heavy metals

Anodic electrochemically active biofilms

BES

Microbial community

ABSTRACT

Heavy metals play an important role in the conductivity of solution, power generation and activity of microorganisms in bioelectrochemical systems (BESs). However, effect of heavy metal on the process of exoelectrogenesis metabolism and extracellular electron transfer of electrochemically active biofilms (EABs) was poorly understood. Herein, we investigated the impact of Cu^{2+} at gradually increasing concentration on the morphological and electrochemical performance and bacterial communities of anodic biofilms in mixed-culture BESs. The voltage output decreased continuously and dropped to zero at 10 mg L^{-1} , which was attributed to the toxic inhibition that caused anodic biofilm damage and decreased secretion of outer membrane cytochromes. When stopping the introduction of Cu^{2+} to anodic chamber, the maximum voltage production recovered 75.1% of the voltage produced from BES and coulombic efficiency was higher but acetate removal rate was lower than that before Cu^{2+} addition, demonstrating the recovery capability of EABs was higher compared to nonelectroactive bacteria. Moreover, SEM-EDS and XPS suggested that most of Cu^{2+} was adsorbed by the anode electrode and reduced by EABs on anode. Compared to the open-circuit BES, the flow of electrons through a circuit could improve the reduction of copper. Community analysis showed a decrease in *Geobacter* accompanied by an increase in *Stenotrophomonas* in response to Cu^{2+} shock in anodic chamber.

© 2018 Elsevier Ltd. All rights reserved.

1. Introduction

Wastewater containing various dissolved heavy metals from mining, electroplating and many manufacturing industries was one

* Corresponding author.

E-mail address: yuanyong@soil.gd.cn (Y. Yuan).

of the trickiest pollution to deal with and presented a serious danger to public health and environment because of its toxicity, non-biodegradability and bio-accumulation (Fu and Wang, 2011; Gall et al., 2015; Gao et al., 2017). Various technologies had been used to remove heavy metals from these industrial wastewaters, including physical reduction (Aflaki et al., 2016; Zhang et al., 2016), chemical reduction (Seaman et al., 1999), biological reduction (Wang et al., 2013) and the comprehensive applications of these methods (Ntagia et al., 2016; Sulaymon et al., 2016; Víctor-Ortega et al., 2016; Yang et al., 2016). Among these methods, BESs had attracted more attention as effective and sustainable technologies for the reduction of heavy metals (Zhang et al., 2012; Wang and Ren, 2014). BESs characterized itself by adopting electrochemically active bacterium (EABs) as biocatalyst to facilitate energy conversion from the chemical energy of organics into electricity (Lovley, 2008; He et al., 2015). In earlier BESs studies, heavy metals removal had been studied in abiotic cathode chamber due to the comparable oxidation-reaction potential of the most heavy metals to that of oxygen reduction (Heijne et al., 2010; Zhang et al., 2015; Wu et al., 2016). Thermodynamically, heavy metal served as electron acceptor in catholyte was feasible, and the reduction process could occur spontaneously. In parallel, the organic matter was used as an electron donor in anode chamber (Heijne et al., 2010; Miran et al., 2017). Subsequently, the development of biocathodic-BESs had been shown to be efficient in the reduction of heavy metals (Venkata Mohan et al., 2014; Huang et al., 2015; Li et al., 2016a; Nancharaiah et al., 2016). Nevertheless, in these studies, only heavy metals without organic matter were introduced to cathode chamber, however, heavy metals were usually found to coexist always with organics in actual wastewater such as printing, animal farms, textile and other industrial wastewater (Pathak et al., 2009; Ghosh et al., 2011), and also exist in water treatment chemicals such as alum, in which the toxicity of alum had been detected using MFC sensors (Li et al., 2016b). Recently, Abourached et al. (2014) discovered that high Cd (90%) and Zn (97%) and organic matter removal efficiencies were obtained simultaneously in the anodic chamber of BES, and heavy metals concentration was inversely correlated with voltage output of BES, which demonstrated the toxicity suppression of anodic microbes due to the incremental increase in Zn and Cd concentrations. Feng et al. (2013) found the high concentration of Cu^{2+} would deteriorate the effluent quality and inhibit the voltage production, and the ability to treat wastewater and voltage was restored after a period around 30 d. However, how the electrons transferred in the presence of heavy metal, the suppression mechanism, viability and species composition of microorganism were unclear.

Heavy metals played significant roles in the physiological process of microbial cells, such as free radical defense, enzymes involved in cellular respiration, connective tissue biosynthesis and other process (de Oliveira-Filho et al., 2004). We also known that heavy metals in water bodies at excessive concentrations could cause adverse ecotoxicological effects and were accumulated primarily by adsorbed on extracellular polymeric substances (EPS) from the substrates, adsorbed on cell surface and then intracellular uptake into the cytosol (Holding et al., 2003; Haferburg and Kothe, 2010). Guo et al. (2017) found that the residual heavy metals might result in the denaturation and inactivation of enzymes, rupture of membrane integrity and organelles (Alexandrino et al., 2011), and subsequently inhibit the metabolism of biofilms. Cabrera et al. (2006) studied toxic inhibition of heavy metals through evaluating the precipitation of heavy metals on sulfate-reducing bacteria. However, the process of inhibitory effect on biofilms of heavy metals in the above studies is different from that on EABs, in which the extracellular electron transfer (EET) process and metabolic pathway and environment matrix is more complicated. Specifically, in the anodic chamber, the

organic matter oxidation was carried out by microorganism, while electrons passed to the anode from their metabolism (Bond and Lovley, 2003; Srikanth et al., 2008; Saratale et al., 2017). The dissimilatory metal-reducing bacterial, which was also found in EABs from BESs, could respire on multiple metals ions (Tian et al., 2017). Therefore, when heavy metal was introduced to anodic chamber, electrons from organic matter could be transferred to heavy metal ions or anodic electrode. In the presence of such a multiple electron acceptor, the competition of electron between heavy metals and anode electrode may become even more complicated. The understanding of electron transfer competition mechanism between heavy metal ions or anodic electrode was warranted. Moreover, relatively less effort had been devoted to the in-depth analysis of the observed inhibition (Abourached et al., 2014). There was a need for investigating the response of the microbial viability and communities to perturbations of heavy metal. In addition, heavy metals nano-particles deposited on the surface of graphite felt through reduction process may affect the anode performance (Tian et al., 2017), which also may result in forming good conductor of these metal deposition in a long-running transaction.

In this study, the reproducibility of the BES was confirmed by running multiple consecutive cycles at a specific anolyte. Cu^{2+} was selected as a representative heavy metal to be introduced to anodic chamber, since its frequent observation in various industrial wastewater (Soares and Soares, 2012; García et al., 2014). The BESs were constructed to investigate EABs-driven anodic reduction of Cu-loaded anolyte by examining the changes in concentrations of Cu^{2+} as a function of anodic microorganism response, including the shift of viability and species composition of microorganism, utilized by confocal laser scanning microscopy (CLSM) and the Illumina Miseq platform. In addition, the anodic redox reactions in the presence of Cu^{2+} and anode electrode for multiple electron acceptor were further disclosed by performing cyclic voltammetry (CV). SEM-EDS and XPS were also conducted to observe morphological structure of the copper precipitates on bioanode for various concentration of Cu-loaded anolyte in anodic chamber.

2. Materials and methods

2.1. BES design and operation

A dual chamber BES was arranged, with a cylindrical chamber 2.4 cm long by 4.9 cm in diameter from a plastic transparent cube. Graphite felt electrodes ($2.5 \times 3.0 \times 0.5$ cm) were twined with titanium wire and were glued to the upper end of the anode and cathode compartments, respectively. A cation exchange membrane (18.8 cm^2 working surface area) was placed between the two chambers to maintain electroneutrality. The BESs were operated at a fixed external resistance of 510Ω for electron transfer and completed the circuit. All of the reactors were conducted in a thermostats (28°C).

The bioanode was inoculated with suspended mixed anaerobic culture collected from sewage sludge with sodium acetate as the electron donor. The microbes grew on the bioanode, which submerged in the nutrient solution contained (per L): 1 g sodium acetate, 15.1 g PIPES buffer, 0.31 g NH_4Cl , 0.13 g KCl, 12.5 mL trace elements, 5 mL vitamins (Liu and Logan, 2004; Abourached et al., 2014). The bioanode was acclimated in fed-batch mode for about 3 weeks when the electricity was stable for at least three refreshment cycles, and anolyte was refreshed in 3 or 4 days. The cathodic chamber was filled with 50 mM $\text{K}_3[\text{Fe}(\text{CN})_6]$ and 50 mM PIPES buffer, ensuring that the terminal electron acceptor concentration would not be a limit factor. All of the cathode chambers were wrapped with black insulation tape to exclude light to prevent the decomposition of $\text{K}_3[\text{Fe}(\text{CN})_6]$.

Several sets of BESs were operated for different purposes. The

first reactor, as heavy metals blank test, sequentially operated with the nutrient solution above for continual electricity. The heavy metal concentrations were increased gradually in an increment of 5 mg L^{-1} for the second BES, the addition of heavy metal continued to mount up until the maximum voltage output nearly was 0.01 V , then filled anode compartment with the same solution except heavy metal to evaluated the recovery situation of voltage. To further elucidate the effect of microorganisms on the reduction of Cu^{2+} , abiotic control was performed under identical conditions. Additionally, open-circuit BES was also performed to discuss the effect of current on reduction of Cu^{2+} .

2.2. Measurements and analyses

The voltages across the external resistance were monitored every 10 min using an automatic data acquisition installation (2700, Keithley, USA). The acetate concentration was measured by ion chromatograph (ICS-900, Daian, USA). For residual soluble Cu^{2+} concentration in the anolyte effluent, which were filtered through $0.45 \mu\text{m}$ membrane syringe filters, were determined by atomic absorption spectroscopy. Coulombic efficiency was determined by the ratio of total recovered coulombs to the theoretical amount of coulombs from acetate (Liu and Logan, 2004). Power densities and polarization curves of the BESs were examined by the gradual lowering of the external resistor from 1000 to 50Ω using a resistance box (Qiao et al., 2008). To examine the bioelectrochemical behavior of anodic biofilms, the CV was carried out in a three-electrode system with the anode as a working electrode, the cathode as a counter electrode, and a saturated calomel electrode as reference electrode inserting into the anodic compartment. CV was run with the potential between -0.6 and $+0.5 \text{ V}$ at a scan rate of 1 mV s^{-1} . At the end of the reactors operation, the anodes and the CEMs were sampled for further studies to inspect the transportation and transformation of the heavy metal in the BESs. A scanning electronic microscopy (SEM) coupled with an energy dispersive X-ray spectrometer (EDS) was used to examine the biofilm surface morphologies and elemental compositions before and after Cu^{2+} reduction. X-ray photoelectron spectroscopy (XPS) was conducted to detect deposited copper or other valence of copper ions on the anode and CEM. Further, biofilms from anode were also examined by CLSM to analyse an adverse reaction to the heavy metals.

To analyse the component of bioanode, the biofilm samples were collected from graphite felts of the anodes in BESs supplied with different Cu^{2+} concentrations. The genomic DNA was extracted using E.Z.N.A™ Mag-Bind Soil DNA Kit (Omega Bio-Tek, USA). DNA concentration was determined using Qubit 3.0 fluorometer (Invitrogen, Shanghai, China). The V3-V4 regions of bacterial 16S rRNA genes were amplified using universal primers 341F (CCCTA-CACGACGCTCTCCGATCTG CCTACGGGNGGCWGCAG) and 805R (GACTGGAGTTCCTTGGACCCGAGAATTCAGACTACHVGGGTATCTA ATCC). PCR amplification was conducted using T100™ Thermal cycler (Bio-Rad, USA). Addition of the compatible primer of Illumina was performed in the second PCR process, and the thermal cycling conditions were set as follows: initial denaturation at $95 \text{ }^\circ\text{C}$ for 3 min, followed by 5 cycles of $94 \text{ }^\circ\text{C}$ for 20 s, $55 \text{ }^\circ\text{C}$ for 20 s and $72 \text{ }^\circ\text{C}$ for 30 s, and finally followed by an extension period at $72 \text{ }^\circ\text{C}$ for 5 min. After purification, paired-end of PCR products was submitted to the Sangon Biotech Co. Ltd (Shanghai, China) for sequencing on an Illumina MiSeq platform.

3. Results and discussion

3.1. Electrochemical performance of the BESs

As shown in Fig. 1a, the voltage production produced by BESs

increased gradually and ran stably for several cycles ($0.62 \pm 0.01 \text{ V}$), indicating that EABs had been acclimated successfully on the anode (Yu et al., 2017). Then, different initial Cu^{2+} concentration were introduced to the anode chamber to determine the response of EABs to Cu^{2+} during multiple parallel batch cycles. The maximum voltage production in each batch run decreased continuously with gradually increasing initial concentration of Cu^{2+} . Specifically, when anode chamber was fed with the solution containing $5 \text{ mg L}^{-1} \text{ Cu}^{2+}$, voltage output ($0.60 \pm 0.02 \text{ V}$) decreased slightly for the first batch run, and for the second and third cycle of 5 mg L^{-1} , the highest voltage production dropped by 37.5% and 54.8%, respectively. These results were possibly due to the toxicity of Cu^{2+} to microbial species. Subsequently, when $10 \text{ mg L}^{-1} \text{ Cu}^{2+}$ was introduced to the anode chamber, the maximum voltage output of the BES instantly dropped to $0.02 \pm 0.03 \text{ V}$, possibly due to the copper accumulation during the foregoing cycles. To test the resilience of the biofilms of anode, Cu^{2+} was removed from the influent to the anode. During the recovery stage, the maximum voltage production were gradually increased and achieved $0.46 \pm 0.01 \text{ V}$, which was only 75.1% of the voltage produced from BES without Cu^{2+} , mainly ascribed to the toxicity of Cu^{2+} which inhibited the viability and reproduction of microorganisms (Sheng et al., 2008; Kamika and Momba, 2011; Abourached et al., 2014). Also, a particular concentration of $10 \text{ mg L}^{-1} \text{ Cu}^{2+}$ was repeatedly added to the BES anodic chamber in our early trials. As shown in Fig. S1, when introducing $10 \text{ mg L}^{-1} \text{ Cu}^{2+}$, voltage output dropped significantly and then for all the cycles of 10 mg L^{-1} , the highest voltage production decreased to $\sim 0 \text{ V}$. No voltage production was observed during two months operation with repeat $10 \text{ mg L}^{-1} \text{ Cu}^{2+}$ addition. All these results suggested that the EABs could not be adaptive to a certain Cu^{2+} concentration but could recover when stopping the introduction of Cu^{2+} to anode chamber.

As shown in Fig. 1b, the maximum power densities of BESs decreased gradually as the BESs anode fed with incrementally Cu^{2+} . The maximum power density of $1.81 \pm 0.06 \text{ W m}^{-2}$ was obtained in BES operated at the control (0 mg L^{-1}), with $1.23 \pm 0.02 \text{ W m}^{-2}$ at 5 mg L^{-1} , which dropped by 32.0% of the control. When introducing $10 \text{ mg L}^{-1} \text{ Cu}^{2+}$ into the anode chamber, the maximum power density declined almost to zero. However, when no copper was introduced, the maximum power density increased, which was 88.4% of the initial power density ($1.60 \pm 0.02 \text{ W m}^{-2}$). These results suggested damage to EABs on anode, which likely caused by Cu^{2+} . Moreover, the polarization curves were plotted to investigate the effect of anode and cathode potentials on the cell voltage output of BESs (Fig. 1c). The anodic potentials instantly increased (from -0.30 ± 0.01 to $-0.09 \pm 0.04 \text{ V}$ on 0 mg L^{-1} , from -0.27 ± 0.01 to $0.09 \pm 0.03 \text{ V}$ on 5 mg L^{-1} , from -0.36 ± 0.01 to $-0.21 \pm 0.01 \text{ V}$ on recovery stage) while the cathodic potentials remained almost unchanged. This indicated that the increase of anode potential was responsible for suppressed cell voltage. These results demonstrated that the association of Cu^{2+} with the anode chamber alters the propensity of anode, resulting in the decrease of BES performance during prolonged operation. It was worth noting that all the anodic electrodes displayed overshoots. The power overshoots in the polarization curves usually indicates that the demand for electrons exceeded the rate of electrons supplied by microbial activity, which resulted in the depletion of electrons and ions in the anolyte (Winfield et al., 2011; Wu et al., 2016; Dong et al., 2017; Shen et al., 2017). As shown in Fig. 1c, when introducing $5 \text{ mg L}^{-1} \text{ Cu}^{2+}$ to the anodic chamber, the overshoot became more obvious compared to $0 \text{ mg L}^{-1} \text{ Cu}^{2+}$, suggesting that the increase of Cu^{2+} was toxic for the EABs and the electron demand could not be maintained. When stopping introducing Cu^{2+} to anodic chamber, the overshoot became weak. This indicated that the inhibition of biofilm by heavy metal was alleviated, which means EABs might have the capacity of

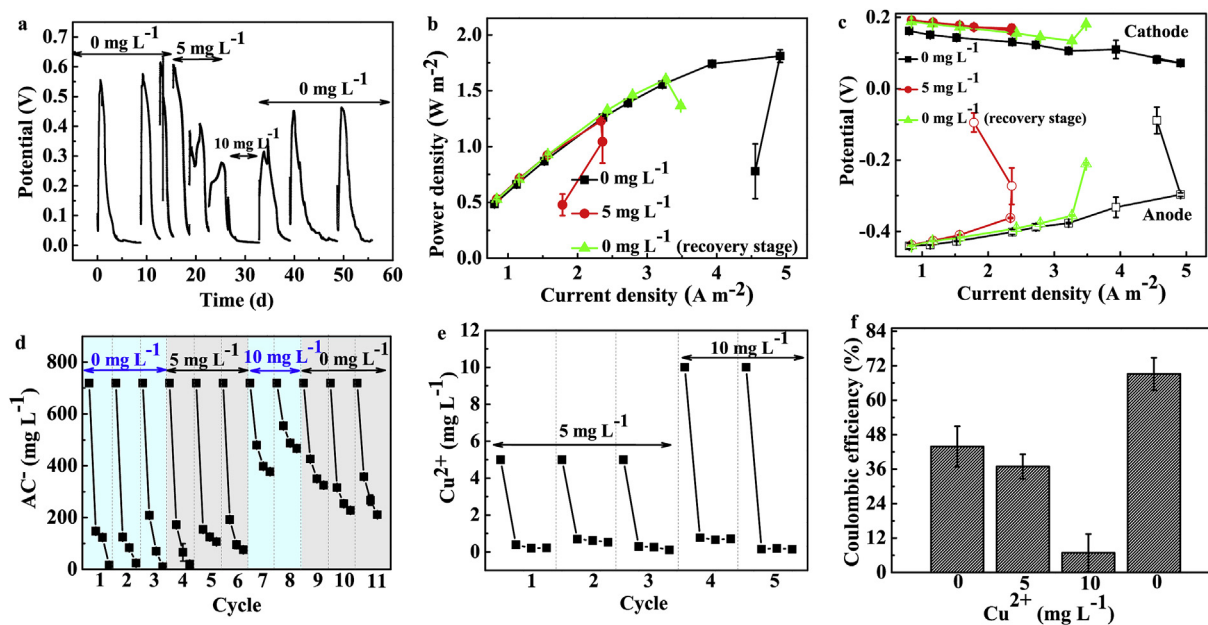


Fig. 1. Effect of the gradual increase in Cu^{2+} concentration on a) voltage output (510 Ω of external resistance), b) power densities and c) polarization curves of anode and cathode. Changes in the remaining concentration of d) AC^- and e) Cu^{2+} in consecutive batch runs conducted with the addition of various initial concentration of Cu^{2+} in anode chamber. f) Anodic coulombic efficacy of BES with addition various initial Cu^{2+} concentrations in anode chamber.

recovering from heavy metals injury.

3.2. The migration and transformation of Cu^{2+}

Samples from anolyte were taken and analyzed three times per cycle. As shown in Fig. 1d, with the increasing concentration of Cu^{2+} , the acetate concentration that can be detected at the end of cycle gradually increased in each batch run. Specially, before Cu^{2+} addition, acetate concentration decreased by 70.9% significantly at first 36 h (from $719.5 \pm 2.8 \text{ mg L}^{-1}$) and continued to decrease to $9.9 \pm 3.0 \text{ mg L}^{-1}$ slowly during next 72 h, with maximum acetate removal rate of 98.6%. And for all the batch runs at $5 \text{ mg L}^{-1} \text{ Cu}^{2+}$, the same degradation trends of acetate was observed, with maximum acetate removal rate of 97.3%. However, when $10 \text{ mg L}^{-1} \text{ Cu}^{2+}$ was introduced, acetate concentration decreased by 33.3% at first 36 h (from 719.5 to $480 \pm 8.8 \text{ mg L}^{-1}$), which was much slower than that of 0 and $5 \text{ mg L}^{-1} \text{ Cu}^{2+}$. The maximum acetate removal rate at $10 \text{ mg L}^{-1} \text{ Cu}^{2+}$ was 47.6%, which was almost 50% lower than that of 0 and $5 \text{ mg L}^{-1} \text{ Cu}^{2+}$. These results were in agreement with the results of the voltages tests, probably due to the inhibition of microorganisms by high concentration of Cu^{2+} (Abourached et al., 2014). To test the resilience of degradation and utilization of acetate by microorganism, Cu^{2+} was removed from the influent to the anode. During the first 36 h, acetate concentration decreased by 50.2% (from 719.5 to $358.0 \pm 11.9 \text{ mg L}^{-1}$), which was higher than that of $10 \text{ mg L}^{-1} \text{ Cu}^{2+}$ but still lower than that of 0 and $5 \text{ mg L}^{-1} \text{ Cu}^{2+}$. The maximum acetate removal rate of 70.7% was obtained, which was lower than that of 0 and $5 \text{ mg L}^{-1} \text{ Cu}^{2+}$. This result suggested that the ability of BES anode to degrade substrate was resilient to Cu^{2+} strike (Feng et al., 2013).

Similar to the acetate degradation, Cu^{2+} concentration decreased instantly during the first 36 h and showed a steady decrease after 72 h (Fig. 1e). During each treatment cycle in BES, Cu^{2+} was almost completely removed under various initial Cu^{2+} concentrations. The maximum removal rate of 97.8% (with effluent concentration of $0.11 \pm 0.06 \text{ mg L}^{-1}$) was obtained under the

influent concentration of 5 mg L^{-1} . Notably, when no voltage was produced under the influent concentration of 10 mg L^{-1} , the maximum Cu^{2+} removal rate of 98.5% was obtained with the effluent concentration of $0.15 \pm 0.02 \text{ mg L}^{-1}$. The high Cu^{2+} degradation might be ascribed to the adsorption by the graphite felt of anode electrodes and cation exchange membrane (Abourached et al., 2014), and direct reduction by microorganisms in the anode chamber. To examine the contribution of the current produced from organics oxidation in the anode chamber, the coulombic efficiency (CE) were also calculated (Liu and Logan, 2004) and were showed in Fig. 1f. The CE value of $43.8 \pm 7.0\%$ was obtained when the anolyte contained no Cu^{2+} . Subsequently, the CE results of $36.9 \pm 4.2\%$ was observed for BES with addition of $5 \text{ mg L}^{-1} \text{ Cu}^{2+}$. However, the addition of $10 \text{ mg L}^{-1} \text{ Cu}^{2+}$ resulted in an extensive reduction of CE ($6.8 \pm 6.6\%$). The slight change of CE at the $5 \text{ mg L}^{-1} \text{ Cu}^{2+}$ and the significant drop at $10 \text{ mg L}^{-1} \text{ Cu}^{2+}$ suggested that Cu^{2+} mainly affected the contribution efficiency of acetate used as electron donors to external circuit current through their toxic inhibition to EABs on anode. At the recovery stage in absence of Cu^{2+} , the CE was 34.0% higher than that before Cu^{2+} addition into anode chamber. While acetate removal rate at the recovery stage was lower than that of initial influent without Cu^{2+} addition (Fig. 1d). These results demonstrated that through toxic inhibition to microorganism of high Cu^{2+} concentration, the recovery capability of EABs was higher compared to the other bacteria. Microorganisms possessed endurance to Cu^{2+} through a various mechanisms due to their habitat sites and capabilities (Huang et al., 2008; Qiu et al., 2009). By comparison with the traditional measures in tackling with wastewaters containing heavy metals, BES had an excellent ability in tolerance, absorption and assimilating heavy metals.

EDS and XPS were conducted to further determine the migration and transformation of copper. As shown in the high-resolution Cu 2p spectra (Fig. 2), the dominant peaks at 932.6 eV and 934.0 eV can be observed on both of graphite felt anode and CEM, which could be attributed to the metal copper and divalent copper ion, respectively (Pan et al., 2015). As shown in Fig. 2a, metal copper (83.4% of the total copper species) was dominant on the anode of

the BES fed with Cu^{2+} concentration of 5 mg L^{-1} . It was noteworthy that small amount of metal copper was also detected on the CEM in this system, likely originating from the reduction of Cu^{2+} by the suspended microorganisms or biofilm-attached on CEM (Fig. 2b). Similarly, metal copper (82.3% of the total copper species on the anode) was dominant on the anode of the BES fed with 10 mg L^{-1} of Cu^{2+} (Fig. 2c). On the contrary, only Cu^{2+} was detected on the graphite electrode and CEM in abiotic control (Fig. 2d and e), resulting from the adsorption. Based on this observation, it was speculated that most of the Cu^{2+} was reduced to Cu through a bioelectrochemical process and precipitated in the BES, resulting in a high copper removal. Additionally, open-circuit BES was performed to discuss the effect of current to the reduction of Cu^{2+} . XPS analysis results indicated that in open-circuit BES, metal copper (72.7% of the total copper species on the anode) was detected on the graphite felt of anode electrode (Fig. 2f), which was lower than those on the anode (83.4%) in closed circuit condition (Fig. 2a), indicating that the flow of electrons through a circuit could improve reduction of copper on anode. We speculated that the improved microbial extracellular electron transfer (EET) efficiency enhanced the reduction of copper. Electron acceptor redox potential was considered to be a key factor in determining microbial metabolism and consequent microbial EET (Liu et al., 2010; Wu et al., 2013). In this study, $\text{K}_3[\text{Fe}(\text{CN})_6]$ with a relatively high redox potential was used as acceptor, which was favorable to the electrons transfer from anode to cathode. Therefore, in closed-circuit BES the microbial EET efficiency was high, which was beneficial to the reduction of Cu^{2+} . While in open-circuit BES, there was no electrons flow between anode and cathode, which probably decreased the microbial EET efficiency and consequently was unfavorable to the reduction of Cu^{2+} . EDS measurements also confirmed the presence of copper species on the anode and CEM of the BESs operated in closed and open circuits (Fig. 3d–g).

3.3. Morphological and electrochemical characterizations of anodic biofilms

SEM analysis was conducted to examine the differences in the surface morphology of the anode biofilms under various Cu^{2+} concentration in influent. Fig. 3a showed the SEM images of the bare graphite felt with porous carbon fibers, which is favorable for attaching and growth of microorganisms. After the BES was successfully started up, the surface of carbon fiber had been covered with biofilm, displayed in small-sized and fine-grained granules surface (Fig. 3b). When Cu^{2+} was introduced in anode chamber, diverse copper nanoparticles were found on the surface of the anode (Fig. 3c), demonstrating the greater adsorption and reduction capacity of EABs.

The variations in biofilm viability were further examined by CLSM. Fig. 3h–j showed and compared the CLSM images of the anode biofilms obtained from different concentrations of Cu^{2+} , differentiating the metabolically active (green) and dead cells (red). It was evident that more living cells appeared on the anode surface at 0 mg L^{-1} Cu^{2+} (Fig. 3h). While Cu^{2+} concentration of 5 and 10 mg L^{-1} were introduced to the anode chamber separately, it was clear that more damaged cells were observed on the anode surface at 10 mg L^{-1} Cu^{2+} (Fig. 3j). The relative viability of the biofilms was obtained by calculating the ratio of green fluorescence to the total of red and green fluorescence. The 0 mg L^{-1} Cu^{2+} -fed reactor exhibited a viability value of $80.61 \pm 0.24\%$, demonstrating that the overwhelming majority of the anode biofilms were covered with living cells. When the Cu^{2+} concentration in influent increased to 5 and 10 mg L^{-1} separately, the viability value of $63.5 \pm 5.40\%$ and $47.0 \pm 8.80\%$ were obtained, respectively. These results indicated the toxic inhibition of Cu^{2+} to microorganism gradually increased with the increase of Cu^{2+} concentration, resulting in more cell death. The CLSM results were in good agreement with the voltage

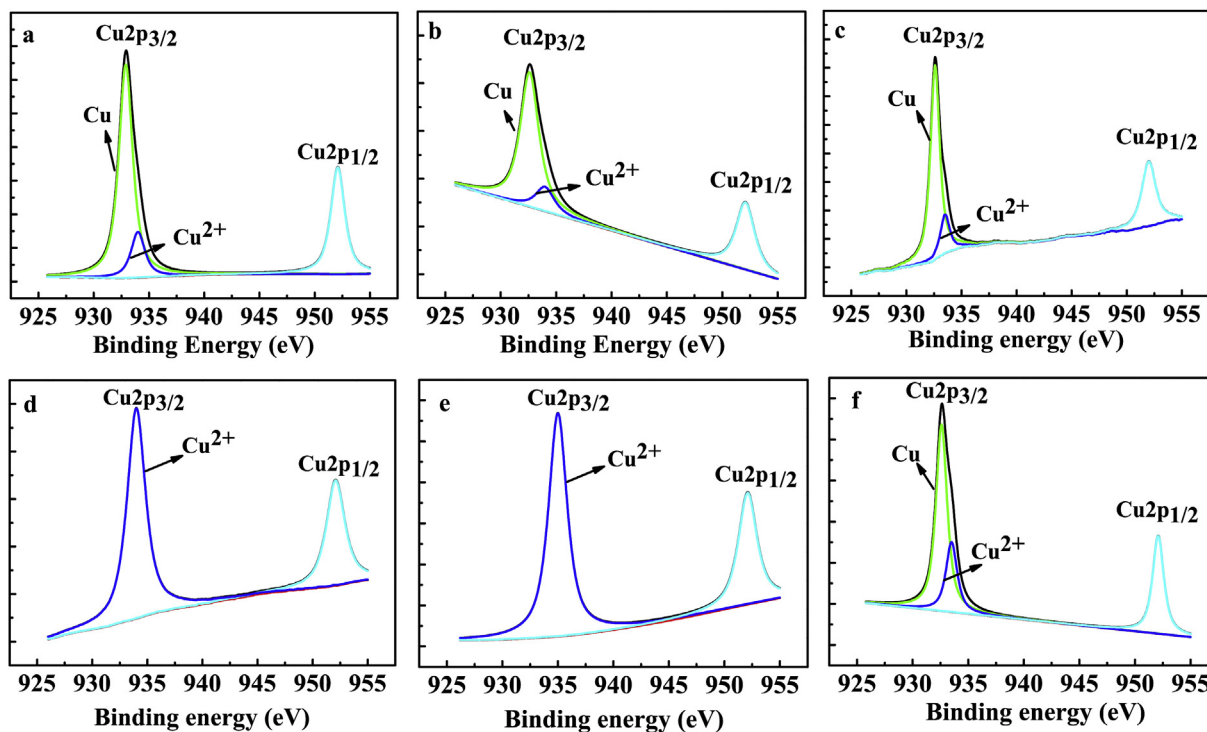


Fig. 2. XPS spectra of Cu precipitates on the graphite felt bioanode with the addition of a) 5 mg L^{-1} Cu^{2+} and c) 10 mg L^{-1} Cu^{2+} in closed circuit; on the CEM with the addition of b) 5 mg L^{-1} Cu^{2+} in closed circuit; on the d) abiotic graphite felt anode and e) abiotic CEM with the addition of 5 mg L^{-1} Cu^{2+} in closed circuit; f) on the graphite felt bioanode with the addition of 5 mg L^{-1} Cu^{2+} in open circuit BES.

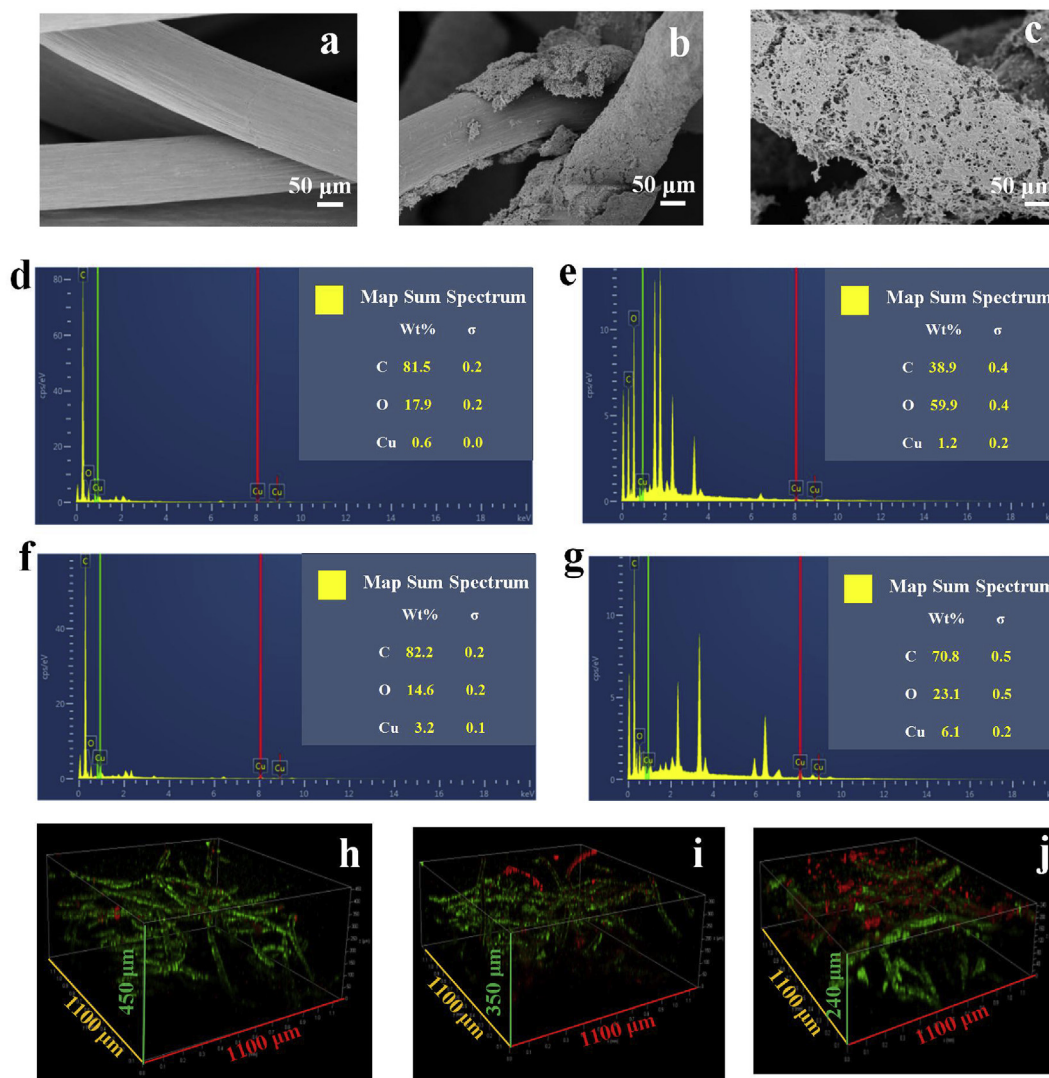


Fig. 3. SEM images of a) the graphite felt; b) the microorganism grown on the graphite felt anode and c) the microorganism of anode with the Cu^{2+} addition; EDS analysis on products of Cu^{2+} reduction on the d) graphite felt anode and e) CEM with the addition of Cu^{2+} at the closed circuit operation; on the f) graphite felt anode and g) CEM with the addition of Cu^{2+} at the open circuit operation. 3D structure images of anode biofilms were observed by CLSM with addition of h) $0 \text{ mg L}^{-1} \text{ Cu}^{2+}$, i) $5 \text{ mg L}^{-1} \text{ Cu}^{2+}$ and j) $10 \text{ mg L}^{-1} \text{ Cu}^{2+}$ in anodic chamber.

output data.

To investigate the effect of the different Cu^{2+} concentrations on the catalytic activities of biofilms, CVs of the biofilms on the anodes were performed (Rabaey et al., 2008; Varanasi et al., 2016). As observed in Fig. 4a, upon addition of sodium acetate, a sigmoidal shaped CV was obtained indicative of catalytic oxidation of the acetate by the biofilm and electron transfer to the electrode. Compared to the control (without Cu^{2+} addition), the catalytic current when introducing $5 \text{ mg L}^{-1} \text{ Cu}^{2+}$ to anode chamber did not greatly alter. While the Cu^{2+} concentration increased to 10 mg L^{-1} , the corresponding catalytic current fallen to the lowest level. When stopping the introduction of Cu^{2+} to anodic chamber, the catalytic current recovered. These suggested that the EABs could be inhibited by Cu^{2+} and could be recovered in certain degree by removing Cu^{2+} from the anode.

Furthermore, a more detailed view on the anode electrochemical features of the biofilm were obtained upon the depletion of substrate. Under these non-catalytic conditions, as illustrated in Fig. 4b, all the anodes showed one major redox system, at a formal

potential of -0.33 V vs. SCE at either 0 or $5 \text{ mg L}^{-1} \text{ Cu}^{2+}$. When $10 \text{ mg L}^{-1} \text{ Cu}^{2+}$ was introduced, no redox peaks was observed. The shape and redox potential were nearly identical to other electroactive biofilms found in other studies (Fricke et al., 2008; Katuri et al., 2010). The redox peaks were resulted from outer membrane cytochromes, which were vital to EET in BES (Liu et al., 2008). The disappearance of the redox peaks when introducing $10 \text{ mg L}^{-1} \text{ Cu}^{2+}$ in influent may be ascribed to the high concentration of Cu^{2+} that inhibited the secretion of outer membrane cytochromes by EABs. When Cu^{2+} removed from influent, the redox peaks was observed again, suggesting that the EABs recovered to secrete outer membrane cytochromes and resulted in the increase of EET rate after Cu^{2+} shock.

3.4. Analysis of bacterial communities in the anodic biofilms

In order to investigate the bacteria community changes influenced by the Cu^{2+} shock in the anode, approximately 44207 high-quality pyrosequencing reads were obtained from per samples on

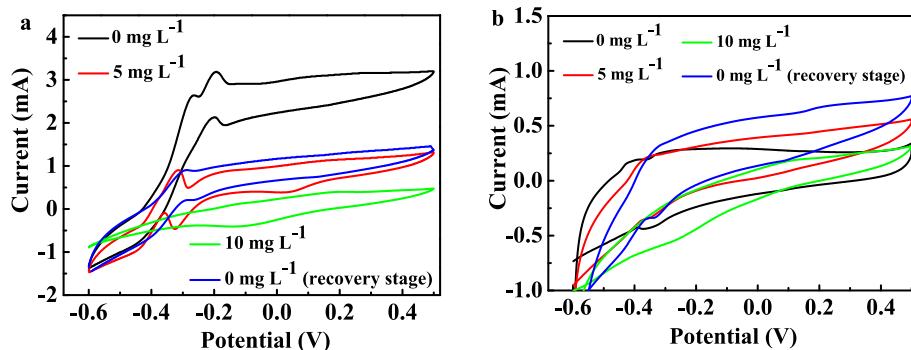


Fig. 4. a) CV curve with substrates addition of BES anode at various initial concentration of Cu^{2+} , with a scanning rate of 1 mV s^{-1} ; b) CV curve without substrates addition of BES anode at various initial concentration of Cu^{2+} , with a scanning rate of 1 mV s^{-1} .

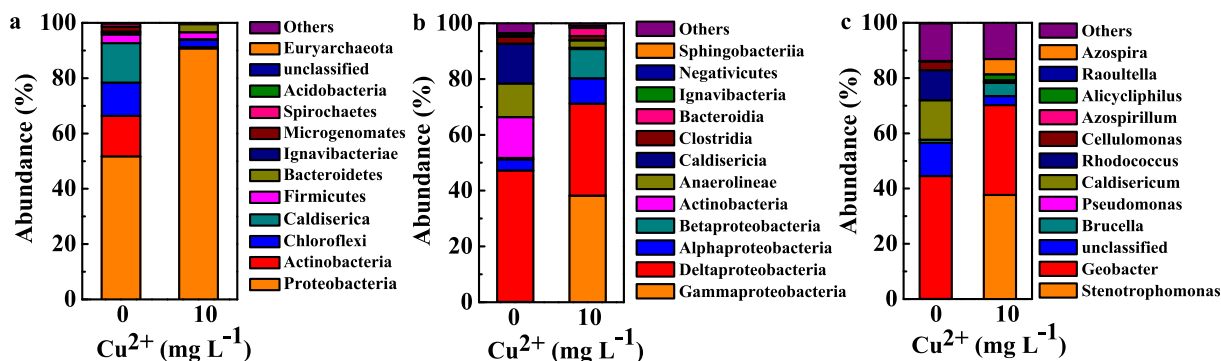


Fig. 5. The comparison of microbial communities on the anode of BESs with and without Cu^{2+} addition at the a) phyla level, b) class level and c) genus level.

the anodes in BESs (Fig. 5). For the anode of 0 and $10 \text{ mg L}^{-1} \text{ Cu}^{2+}$, the most dominant phyla were *Proteobacteria*, *Actinobacteria*, *Chloroflexi* and *Caldiserica*. The abundance of *Proteobacteria* increased from 51.7% to 90.7% after high level of Cu^{2+} exposure. The percentage of *Actinobacteria*, *Chloroflexi* and *Caldiserica* decreased in the anodic biofilm sample after high level of Cu^{2+} shock (Fig. 5a). On the basis of class analysis, the abundance of *Gammaproteobacteria*, *Alphaproteobacteria* and *Betaproteobacteria* increased, and the percentage of *Deltaproteobacteria*, *Actinobacteria* and *Anaerolineae* decreased (Fig. 5b). As for the genus level, the abundance of *Geobacter* decreased from 44.5% to 32.5%, while the percentage of *Stenotrophomonas* significantly increased from 0.03% to 37.7% (Fig. 5c). *Geobacter* species had been found to be significant agents for the bioremediation of wastewater contaminated with toxic metals (Holmes et al., 2002; Ortiz-Bernad et al., 2004). The physiological characteristic of the *Geobacter* species was their capacity to oxidize organic matter, transferring the electrons onto extracellular electron acceptors such as toxic metals (Loneragan et al., 1994; Ortiz-Bernad et al., 2004) and electrodes (Bond et al., 2002). The percentage decrease of *Geobacter* corresponded to the results that voltage production decreased as introduction of Cu^{2+} . *Stenotrophomonas* was known to convert Cu^{2+} into Cu on the surface of anode (Ye et al., 2013; Chen et al., 2016). In addition, *Stenotrophomonas* can tolerate high concentrations of metals (Chien et al., 2007; Ryan et al., 2009). The changes of microbial community composition after high level of Cu^{2+} exposure were mainly ascribed to that high level of Cu^{2+} pollution could exert a selective shock on the microbial community and lead to the emergence of resistant strains (Lasat, 2002; Wang et al., 2007). Diversity indices were calculated with 2600 re-sampling reads per sample may have an effect on diversity (Gihring et al., 2012). In total, 5184 OTUs were identified based on the 97% identity cut-off, with 2731 and 2453

OTUs recovered from anode samples of 0 and $10 \text{ mg L}^{-1} \text{ Cu}^{2+}$, respectively.

4. Conclusion

This study demonstrated the changes in concentrations of Cu^{2+} as a function of anodic microorganism response in the EABs-driven anode chamber, in which heavy metals and organic matter existed simultaneously. We suggested that heavy metals with high concentration would show toxic effects to bioanode, which could subsequently have an adverse impact on the power density and voltage production of BES, and restrict the degradation of acetate and reduction of heavy metals. Differences in the abundance of community in response to different concentration of Cu^{2+} were mainly ascribed to that high level of Cu^{2+} pollution that could exert a selective shock on the microbial community and lead to the emergence of resistant strains. When stopping the introduction of Cu^{2+} to anode chamber, it was turned out that the inhibition of biofilm by heavy metal was alleviated, which means EABs might have the capacity of recovering from heavy metals injury. The results in this study added to the in-depth analysis of the observed inhibition on bioanode, and provided new insights into the treatment of organic wastewater containing heavy metals.

Acknowledgments

This work was jointly supported by the National Natural Science Foundation of China (No. 21607030 and 51678162), Natural Science Fund of Guangdong province (No.2016A030310351 and 2016A030313695) and Scientific and Technological Planning Project of Guangzhou, China (201607010318).

Appendix A. Supplementary data

Supplementary data related to this article can be found at <https://doi.org/10.1016/j.chemosphere.2018.01.009>.

References

- Abourached, C., Catal, T., Liu, H., 2014. Efficacy of single-chamber microbial fuel cells for removal of cadmium and zinc with simultaneous electricity production. *Water Res.* 51, 228–233.
- Aflaki, J.M., Dadvand, K.A., Sheykhan, M., 2016. Experimental study of the removal of copper ions using hydrogels of xanthan, 2-acrylamido-2-methyl-1-propane sulfonic acid, montmorillonite: kinetic and equilibrium study. *Carbohydr. Polym.* 142, 124.
- Alexandrino, M., Macias, F., Costa, R., Gomes, N.C., Canario, A.V., Costa, M.C., 2011. A bacterial consortium isolated from an Icelandic fumarole displays exceptionally high levels of sulfate reduction and metals resistance. *J. Hazard Mater.* 187, 362–370.
- Loneragan Jr., C.F., Lovley, D.J., Davis, D.R., Stolz, M., Mcinerney, J.F., 1994. *Geobacter sulfurreducens* sp. nov., a hydrogen- and acetate-oxidizing dissimilatory metal-reducing microorganism. *Appl. Environ. Microbiol.* 60, 3752–3759.
- Bond, D.R., Lovley, D.R., 2003. Electricity production by *Geobacter sulfurreducens* attached to electrodes. *Appl. Environ. Microbiol.* 69, 1548.
- Bond, D.R., Holmes, D.E., Tender, L.M., Lovley, D.R., 2002. Electrode-reducing microorganisms that harvest energy from marine sediments. *Science* 295, 483–485.
- Cabrera, G., Perez, R., Gomez, J.M., Abalos, A., Cantero, D., 2006. Toxic effects of dissolved heavy metals on *Desulfovibrio vulgaris* and *Desulfovibrio* sp. strains. *J. Hazard Mater.* 135, 40–46.
- Chen, S., Yin, H., Tang, S., Peng, H., Liu, Z., Dang, Z., 2016. Metabolic biotransformation of copper-benzo[a]pyrene combined pollutant on the cellular interface of *Stenotrophomonas maltophilia*. *Bioresour. Technol.* 204, 26–31.
- Chien, C.C., Hung, C.W., Han, C.T., 2007. Removal of cadmium ions during stationary growth phase by an extremely cadmium-resistant strain of *Stenotrophomonas* sp. *Environ. Toxicol. Chem.* 26, 664.
- de Oliveira-Filho, E.C., Lopes, R.M., Paumgarten, F.J., 2004. Comparative study on the susceptibility of freshwater species to copper-based pesticides. *Chemosphere* 56, 369–374.
- Dong, Y., Liu, J., Sui, M., Qu, Y., Ambuchi, J.J., Wang, H., Feng, Y., 2017. A combined microbial desalination cell and electro dialysis system for copper-containing wastewater treatment and high-salinity-water desalination. *J. Hazard Mater.* 321, 307–315.
- Feng, C., Hu, A., Chen, S., Yu, C.P., 2013. A decentralized wastewater treatment system using microbial fuel cell techniques and its response to a copper shock load. *Bioresour. Technol.* 143, 76–82.
- Fricke, K., Harnisch, F., Schröder, U., 2008. On the use of cyclic voltammetry for the study of anodic electron transfer in microbial fuel cells. *Energ. Environ. Sci.* 1, 144.
- Fu, F., Wang, Q., 2011. Removal of heavy metal ions from wastewaters: a review. *J. Environ. Manage* 92, 407.
- Gall, J.E., Boyd, R.S., Rajakaruna, N., 2015. Transfer of heavy metals through terrestrial food webs: a review. *Environ. Monit. Assess.* 187, 201.
- Gao, Y., Baisch, P., Mirlean, N., Rodrigues da Silva Junior, F.M., Van Larebeke, N., Baeyens, W., Leermakers, M., 2017. Arsenic speciation in fish and shellfish from the North Sea (Southern bight) and Acu Port area (Brazil) and health risks related to seafood consumption. *Chemosphere* 191, 89–96.
- García, V., Häyrynen, P., Landaburu-Aguirre, J., Piriñá, M., Keiski, R.L., Urriaga, A., 2014. Purification techniques for the recovery of valuable compounds from acid mine drainage and cyanide tailings: application of green engineering principles. *J. Chem. Technol. Biotechnol.* 89, 803–813.
- Ghosh, P., Samanta, A.N., Ray, S., 2011. Reduction of COD and removal of Zn²⁺ from rayon industry wastewater by combined electro-Fenton treatment and chemical precipitation. *Desalination* 266, 213–217.
- Gihring, T.M., Green, S.J., Schadt, C.W., 2012. Massively parallel rRNA gene sequencing exacerbates the potential for biased community diversity comparisons due to variable library sizes. *Environ. Microbiol.* 14, 285–290.
- Guo, J., Kang, Y., Feng, Y., 2017. Bioassessment of heavy metal toxicity and enhancement of heavy metal removal by sulfate-reducing bacteria in the presence of zero valent iron. *J. Environ. Manage* 203, 278–285.
- Haferburg, G., Kothe, E., 2010. Microbes and metals: interactions in the environment. *J. Basic Microb* 47, 453–467.
- He, C.S., Mu, Z.X., Yang, H.Y., Wang, Y.Z., Mu, Y., Yu, H.Q., 2015. Electron acceptors for energy generation in microbial fuel cells fed with wastewaters: a mini-review. *Chemosphere* 140, 12–17.
- Heijne, A.T., Liu, F., Rv, W., Weijma, J., Buisman, C.J., Hamelers, H.V., 2010. Copper recovery combined with electricity production in a microbial fuel cell. *Environ. Sci. Technol.* 44, 4376.
- Holding, K.L., Gill, R.A., Carter, J., 2003. The relationship between epilithic periphyton (biofilm) bound metals and metals bound to sediments in freshwater systems. *Environ. Geochem. Health* 25, 87–93.
- Holmes, D.E., Finneran, K.T., O'Neil, R.A., Lovley, D.R., 2002. Enrichment of members of the family *Geobacteraceae* associated with stimulation of dissimilatory metal reduction in uranium-contaminated aquifer sediments. *Appl. Environ. Microbiol.* 68, 2300–2306.
- Huang, H.L., Shih, H.Y., Lee, C.M., Yang, T.C., Lay, J.J., Lin, Y.E., 2008. In vitro efficacy of copper and silver ions in eradicated *Pseudomonas aeruginosa*, *Stenotrophomonas maltophilia* and *Acinetobacter baumannii*: implications for on-site disinfection for hospital infection control. *Water Res.* 42, 73–80.
- Huang, L., Wang, Q., Jiang, L., Zhou, P., Quan, X., Logan, B.E., 2015. Adaptively evolving bacterial communities for complete and selective reduction of Cr(VI), Cu(II), and Cd(II) in biocathode bioelectrochemical systems. *Environ. Sci. Technol.* 49, 9914–9924.
- Kamika, I., Momba, M.N., 2011. Comparing the tolerance limits of selected bacterial and protozoan species to nickel in wastewater systems. *Sci. Total Environ.* 410–411, 172–181.
- Katuri, K.P., Kavanagh, P., Rengaraj, S., Leech, D., 2010. *Geobacter sulfurreducens* biofilms developed under different growth conditions on glassy carbon electrodes: insights using cyclic voltammetry. *Chem. Commun.* 46, 4758–4760.
- Lasat, M.M., 2002. Phytoextraction of toxic metals. *J. Environ. Qual.* 31, 109–120.
- Li, C., Yi, X., Dang, Z., Yu, H., Zeng, T., Wei, C., Feng, C., 2016a. Fate of Fe and Cd upon microbial reduction of Cd-loaded polyferric flocs by *Shewanella oneidensis* MR-1. *Chemosphere* 144, 2065–2072.
- Li, T., Wang, X., Zhou, L., An, J., Li, J., Li, N., Sun, H., Zhou, Q., 2016b. Bioelectrochemical sensor using living biofilm to in situ evaluate flocculant toxicity. *ACS Sensors* 1, 1374–1379.
- Liu, H., Logan, B.E., 2004. Electricity generation using an air-cathode single chamber microbial fuel cell in the presence and absence of a proton exchange membrane. *Environ. Sci. Technol.* 38, 4040–4046.
- Liu, Y., Harnisch, F., Fricke, K., Sietmann, R., Schroder, U., 2008. Improvement of the anodic bioelectrocatalytic activity of mixed culture biofilms by a simple consecutive electrochemical selection procedure. *Biosens. Bioelectron.* 24, 1012–1017.
- Liu, H., Matsuda, S., Kato, S., Hashimoto, K., Nakanishi, S., 2010. Redox-responsive switching in bacterial respiratory pathways involving extracellular electron transfer. *ChemSuschem* 3, 1253–1256.
- Lovley, D.R., 2008. The microbe electric: conversion of organic matter to electricity. *Curr. Opin. Biotechnol.* 19, 564–571.
- Miran, W., Jang, J., Nawaz, M., Shahzad, A., Jeong, S.E., Jeon, C.O., Lee, D.S., 2017. Mixed sulfate-reducing bacteria-enriched microbial fuel cells for the treatment of wastewater containing copper. *Chemosphere* 189, 134–142.
- Nancharajah, Y.V., Mohan, S.V., Lens, P.N.L., 2016. Biological and bioelectrochemical recovery of critical and scarce metals. *Trends Biotechnol.* 34, 137–155.
- Ntagia, E., Rodenas, P., Heijne, A.T., Buisman, C., Sleutels, T., 2016. Hydrogen as electron donor for copper removal in bioelectrochemical systems. *Int. J. Hydrogen Energy* 41, 5758–5764.
- Ortiz-Bernad, I., Anderson, R.T., Vrionis, H.A., Lovley, D.R., 2004. Vanadium respiration by *geobacter metallireducens*: novel strategy for in situ removal of vanadium from groundwater. *Appl. Environ. Microbiol.* 70, 3091–3095.
- Pan, L., Ji, Z., Yi, X., Zhu, X., Chen, X., Shang, J., Liu, G., Li, R.W., 2015. Metal-organic framework nanofilm for mechanically flexible information storage applications. *Adv. Funct. Mater.* 25, 2677–2685.
- Pathak, A., Dastidar, M.G., Sreekrishnan, T.R., 2009. Bioleaching of heavy metals from sewage sludge: a review. *J. Environ. Manage* 90, 2343–2353.
- Qiao, Y., Bao, S.J., Li, C.M., Cui, X.Q., Lu, Z.S., Guo, J., 2008. Nanostructured polyaniline/titanium dioxide composite anode for microbial fuel cells. *ACS Nano* 2, 113.
- Qiu, R., Zhao, B., Liu, J., Huang, X., Li, Q., Brewer, E., Wang, S., Shi, N., 2009. Sulfate reduction and copper precipitation by a *Citrobacter* sp. isolated from a mining area. *J. Hazard Mater.* 164, 1310–1315.
- Rabaey, K., Read, S.T., Clauwaert, P., Freguia, S., Bond, P.L., Blackall, L.L., Keller, J., 2008. Cathodic oxygen reduction catalyzed by bacteria in microbial fuel cells. *ISME J.* 2, 519–527.
- Ryan, R.P., Monchy, S., Cardinale, M., Taghavi, S., Crossman, L., Avison, M.B., Berg, G., van der Lelie, D., Dow, J.M., 2009. The versatility and adaptation of bacteria from the genus *Stenotrophomonas*. *Nat. Rev. Microbiol.* 7, 514–525.
- Saratale, G.D., Saratale, R.G., Shahid, M.K., Zhen, G., Kumar, G., Shin, H.S., Choi, Y.G., Kim, S.H., 2017. A comprehensive overview on electro-active biofilms, role of exo-electrogens and their microbial niches in microbial fuel cells (MFCs). *Chemosphere* 178, 534–547.
- Seaman, J.C., And, P.M.B., Schwallie, L., 1999. In Situ Cr(VI) reduction within coarse-textured, oxide-coated soil and aquifer systems using Fe(II) solutions. *Environ. Sci. Technol.* 33, 938–944.
- Shen, J., Huang, L., Zhou, P., Quan, X., Puma, G.L., 2017. Correlation between circual current, Cu(II) reduction and cellular electron transfer in EAB isolated from Cu(II)-reduced biocathodes of microbial fuel cells. *Bioelectrochemistry* 114, 1–7.
- Sheng, Z., Wei, C., Liao, C., Haizhen, W.U., 2008. Damage to DNA of effective microorganisms by heavy metals: Impact on wastewater treatment. *J. Environ. Sci.* 20, 1514.
- Soares, E.V., Soares, H.M., 2012. Bioremediation of industrial effluents containing heavy metals using brewing cells of *Saccharomyces cerevisiae* as a green technology: a review. *Environ. Sci. Pollut. Res. Int* 19, 1066–1083.
- Srikanth, S., Marsili, E., Flickinger, M.C., Bond, D.R., 2008. Electrochemical characterization of *Geobacter sulfurreducens* cells immobilized on graphite paper electrodes. *Biotechnol. Bioeng.* 99, 1065–1073.
- Sulaymon, A.H., Faisal, A.A.H., Khaliefa, Q.M., 2016. Simultaneous adsorption-precipitation characterization as mechanisms for metals removal from aqueous solutions by cement kiln dust (CKD). *Desalin. Water Treat* 57, 819–826.
- Tian, L.J., Li, W.W., Zhu, T.T., Chen, J.J., Wang, W.K., An, P.F., Zhang, L., Dong, J.C., Guan, Y., Liu, D.F., Zhou, N.Q., Liu, G., Tian, Y.C., Yu, H.Q., 2017. Directed

- biofabrication of nanoparticles through regulating extracellular electron transfer. *J. Am. Chem. Soc.* 139, 12149–12152.
- Varanasi, J.L., Nayak, A.K., Sohn, Y., Pradhan, D., Das, D., 2016. Improvement of power generation of microbial fuel cell by integrating tungsten oxide electrocatalyst with pure or mixed culture biocatalysts. *Electrochim. Acta* 199, 154–163.
- Venkata Mohan, S., Velvizhi, G., Annie Modestra, J., Srikanth, S., 2014. Microbial fuel cell: critical factors regulating bio-catalyzed electrochemical process and recent advancements. *Renew. Sust. Energ. Rev.* 40, 779–797.
- Víctor-Ortega, M.D., Ochando-Pulido, J.M., Martínez-Ferez, A., 2016. Thermodynamic and kinetic studies on iron removal by means of a novel strong-acid cation exchange resin for olive mill effluent reclamation. *Eco. Eng* 86, 53–59.
- Wang, H., Ren, Z.J., 2014. Bioelectrochemical metal recovery from wastewater: a review. *Water Res.* 66, 219–232.
- Wang, Y., Shi, J., Wang, H., Lin, Q., Chen, X., Chen, Y., 2007. The influence of soil heavy metals pollution on soil microbial biomass, enzyme activity, and community composition near a copper smelter. *Ecotox. Environ. Safe* 67, 75–81.
- Wang, S., Wang, X., Poon, K., Wang, Y., Li, S., Liu, H., Lin, S., Cai, Z., 2013. Removal and reductive dechlorination of triclosan by *Chlorella pyrenoidosa*. *Chemosphere* 92, 1498–1505.
- Winfield, J., Ieropoulos, I., Greenman, J., Dennis, J., 2011. The overshoot phenomenon as a function of internal resistance in microbial fuel cells. *Bioelectrochemistry* 81, 22–27.
- Wu, C., Cheng, Y.Y., Li, B.B., Li, W.W., Li, D.B., Yu, H.Q., 2013. Electron acceptor dependence of electron shuttle secretion and extracellular electron transfer by *Shewanella oneidensis* MR-1. *Bioresour. Technol.* 136, 711.
- Wu, D., Huang, L., Quan, X., Li Puma, G., 2016. Electricity generation and bivalent copper reduction as a function of operation time and cathode electrode material in microbial fuel cells. *J. Power Sources* 307, 705–714.
- Yang, J., Zhou, M., Hu, Y., Yang, W., 2016. Cost-effective copper removal by electrosorption powered by microbial fuel cells. *Bioprocess. Biosyst. Eng* 39, 511–519.
- Ye, J., Yin, H., Xie, D., Peng, H., Huang, J., Liang, W., 2013. Copper biosorption and ions release by *Stenotrophomonas maltophilia* in the presence of benzo[a]pyrene. *Chem. Eng. J.* 219, 1–9.
- Yu, D., Bai, L., Zhai, J., Wang, Y., Dong, S., 2017. Toxicity detection in water containing heavy metal ions with a self-powered microbial fuel cell-based biosensor. *Talanta* 168, 210–216.
- Zhang, L.J., Tao, H.C., Wei, X.Y., Lei, T., Li, J.B., Wang, A.J., Wu, W.M., 2012. Bioelectrochemical recovery of ammonia-copper(II) complexes from wastewater using a dual chamber microbial fuel cell. *Chemosphere* 89, 1177–1182.
- Zhang, Y., Yu, L., Wu, D., Huang, L., Zhou, P., Quan, X., Chen, G., 2015. Dependency of simultaneous Cr(VI), Cu(II) and Cd(II) reduction on the cathodes of microbial electrolysis cells self-driven by microbial fuel cells. *J. Power Sources* 273, 1103–1113.
- Zhang, Y., Yang, J., Yu, X., 2016. Adsorption technology and mechanism of Cu and CN⁻ from cyanide waste water on modified peanut shell. *Synth. React. Inorg. M.* 46, 561–569.